

## Supplementary Information

# Reducing Undesired Solubility of Squarephaneic Tetraimide for Use as an Organic Battery Electrode Material

Bowen Ding,<sup>a</sup> Manik Bhosale,<sup>b</sup> Troy L.R. Bennett,<sup>a</sup> Martin Heeney,<sup>a,c</sup> Felix Plasser,<sup>d</sup> Birgit Esser,<sup>b\*</sup> and Florian Glöcklhofer<sup>a,e\*</sup>

<sup>a</sup>Department of Chemistry and Centre for Processable Electronics, Imperial College London, Molecular Sciences Research Hub (White City Campus), 80 Wood Lane Shepherd's Bush, London W12 0BZ, United Kingdom

<sup>b</sup>Institute of Organic Chemistry II and Advanced Materials, Ulm University, Albert-Einstein-Allee 11, 89081 Ulm, Germany

<sup>c</sup>Physical Sciences and Engineering Division (PSE), King Abdullah University of Science and Technology (KAUST), Thuwal 23955-6900, Saudi Arabia

<sup>d</sup>Department of Chemistry, Loughborough University, Loughborough LE11 3TU, United Kingdom

<sup>e</sup>Institute of Applied Synthetic Chemistry, TU Wien, Getreidemarkt 9/163, 1060 Vienna, Austria

\*Corresponding Authors: Birgit Esser ([birgit.esser@uni-ulm.de](mailto:birgit.esser@uni-ulm.de)) & Florian Glöcklhofer ([f.glocklhofer@imperial.ac.uk](mailto:f.glocklhofer@imperial.ac.uk), [florian.gloecklhofer@tuwien.ac.at](mailto:florian.gloecklhofer@tuwien.ac.at))

## GENERAL METHODS

UV/Vis data were collected using an Agilent CARY 60 UV/Vis spectrometer, whilst an Agilent Eclipse Fluorescence spectrophotometer was used for the collection of fluorescence data (both interfaced with SCAN software), for samples dissolved in either spectroscopic grade CHCl<sub>3</sub> or DMSO. Elemental analyses were performed through the Elemental Analysis Service Team at London Metropolitan University (United Kingdom), the samples for which were prepared by overnight drying under high vacuum at 120 °C.

## ELECTROCHEMISTRY

Solution and solid state cyclic voltammetry (CV) measurements were conducted with a Metrohm Autolab PGSTAT101 Electrochemical Analyser interfaced to NOVA software. A one compartment three electrode electrochemical cell was used for all measurements, featuring a 7.1 mm<sup>2</sup> glassy carbon working electrode (WE) and a Pt counter electrode. Solid and solution state measurements were conducted in 0.1 M [*n*-Bu<sub>4</sub>N]PF<sub>6</sub>/MeCN and [*n*-Bu<sub>4</sub>N]PF<sub>6</sub>/DMF respectively, with use of an Ag/Ag<sup>+</sup> non-aqueous reference electrode and addition of ferrocene

internal reference. Saturation of the electrolyte with N<sub>2</sub> by bubbling for 20 mins was performed to deoxygenate before measurements were taken. Solid state samples were immobilised onto the WE surface by dipping the electrode into a paste made with MeCN. [n-Bu<sub>4</sub>N]PF<sub>6</sub> for electrochemistry was recrystallized twice in EtOH.

## NUCLEAR MAGNETIC RESONANCE (NMR) SPECTROSCOPY

Solution state <sup>1</sup>H and <sup>13</sup>C NMR spectra were collected on either a Bruker AVANCE 400 or 500 MHz spectrometer. Deuterated CDCl<sub>3</sub> and DMSO-*d*<sub>6</sub> for NMR were obtained from Sigma Aldrich, and their solvent residual signals were used as internal references for chemical shifts (δ).

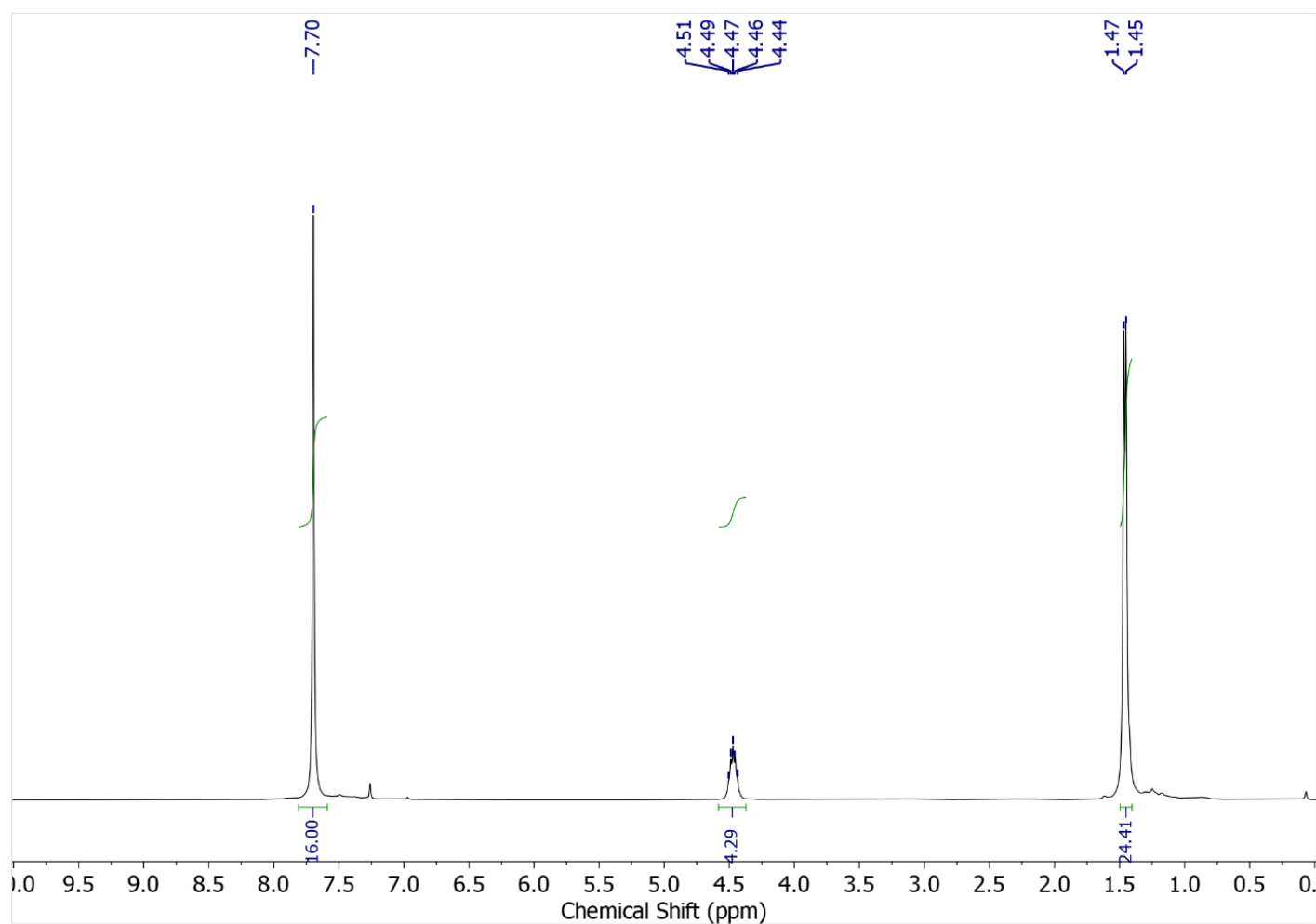


**Figure S1:** <sup>1</sup>H NMR of SqTI-iP in CDCl<sub>3</sub> at 298 K.

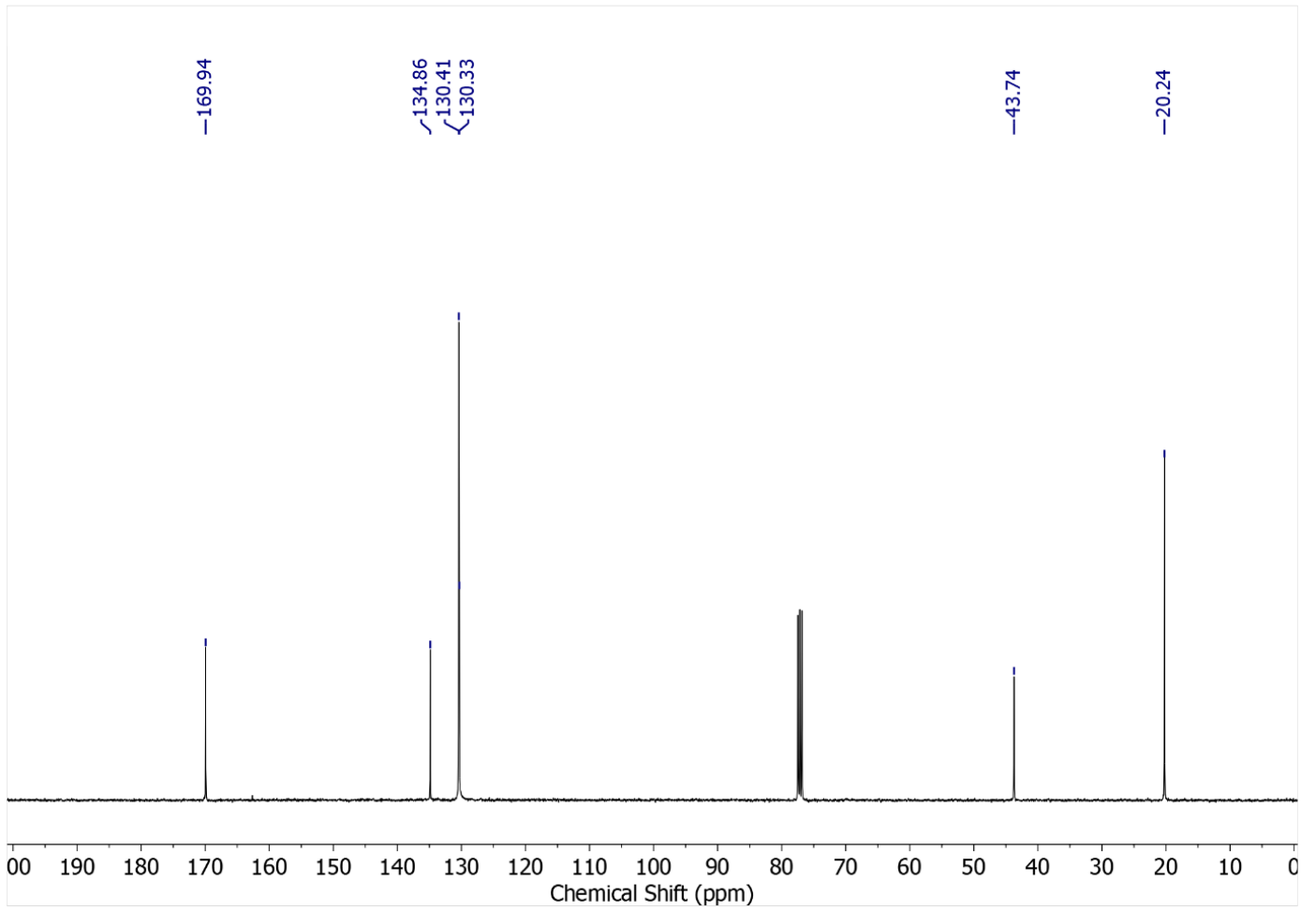


**Figure S2:**  $^{13}\text{C}\{^1\text{H}\}$  NMR of SqTI-iP in  $\text{CDCl}_3$  at 298 K.

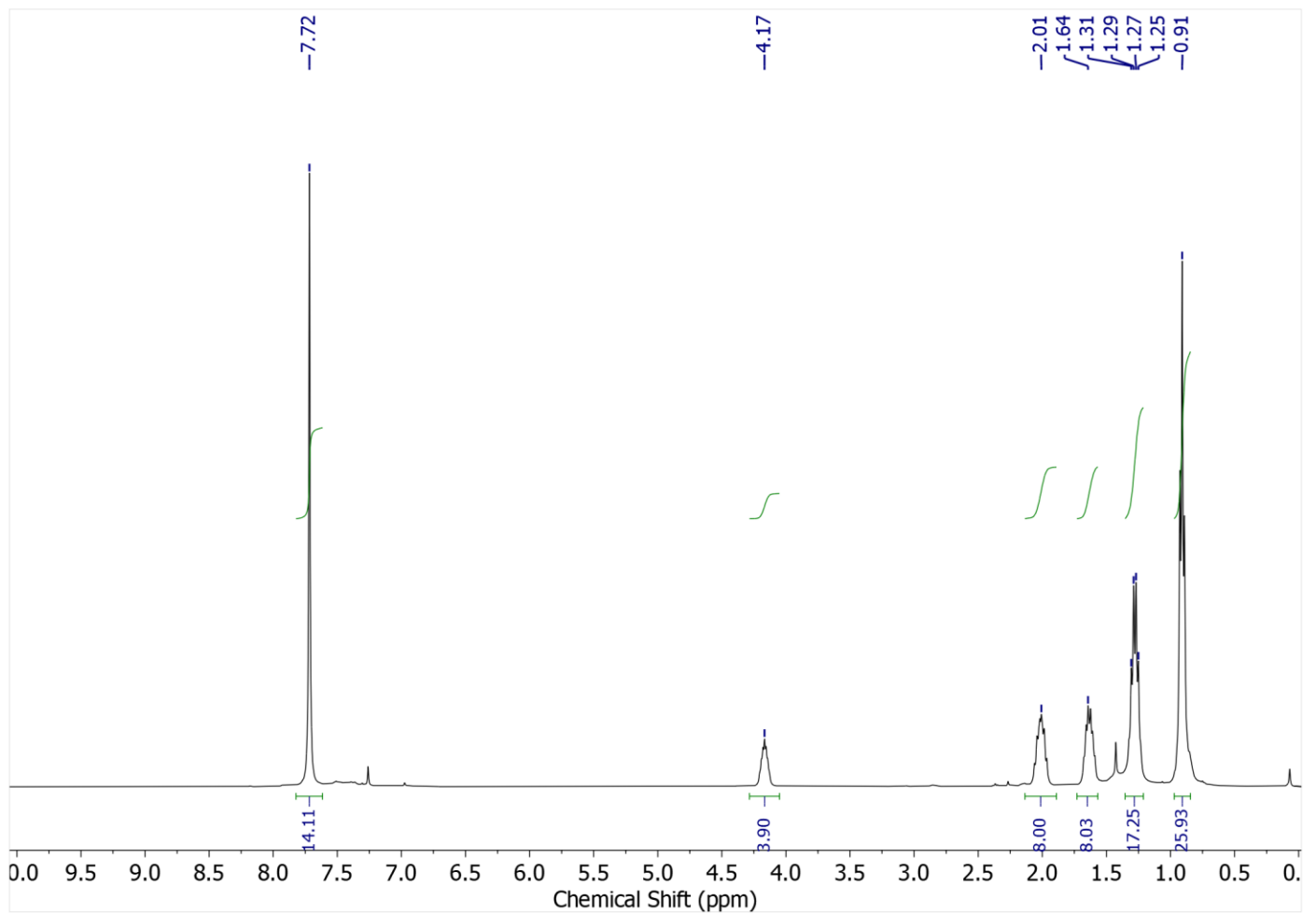


**Figure S3:**  $^1\text{H}$  NMR of SqTI-Hp in  $\text{CDCl}_3$  at 298 K.

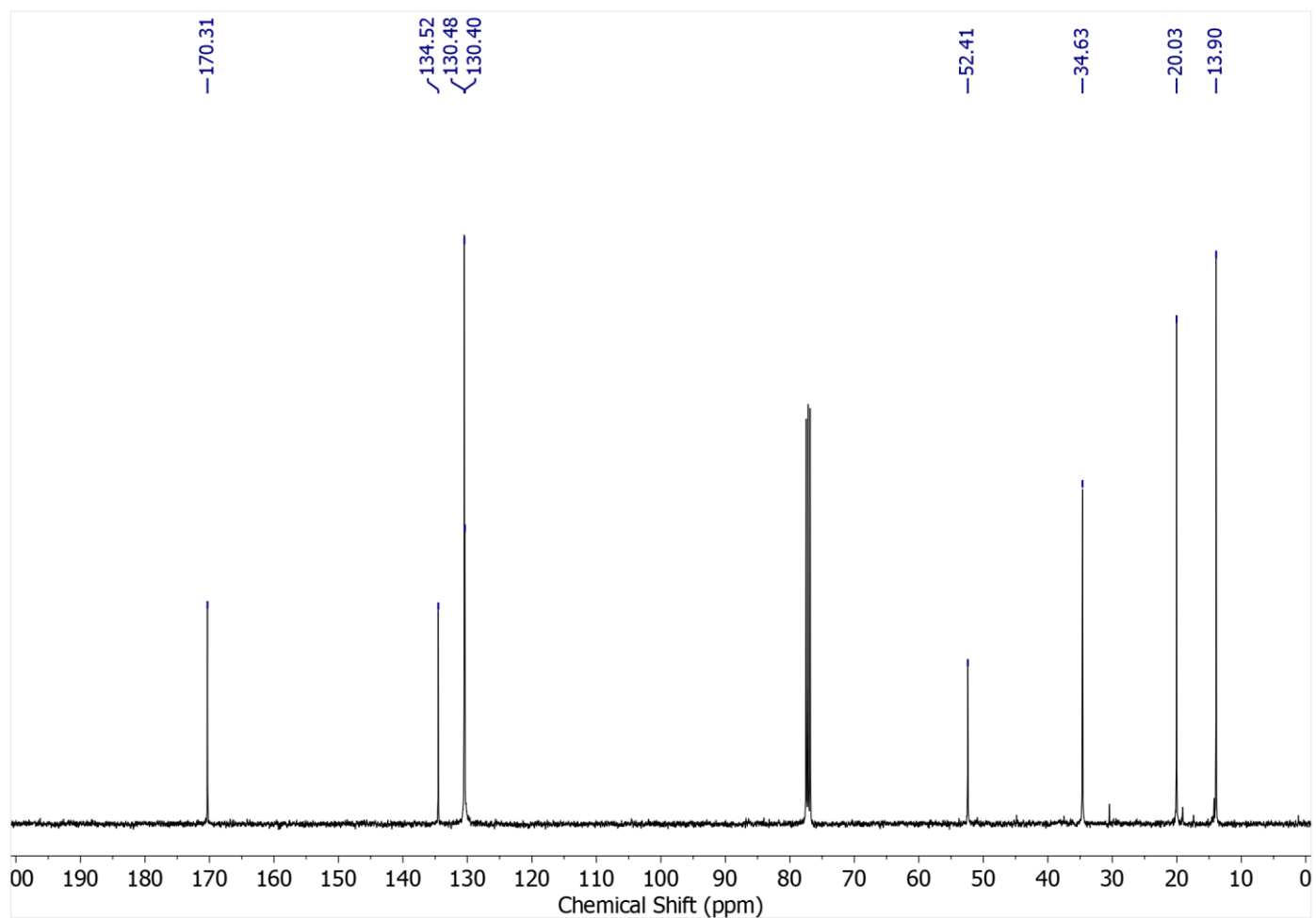


**Figure S4:**  $^{13}\text{C}\{^1\text{H}\}$  NMR of SqTI-Hp in  $\text{CDCl}_3$  at 298 K.

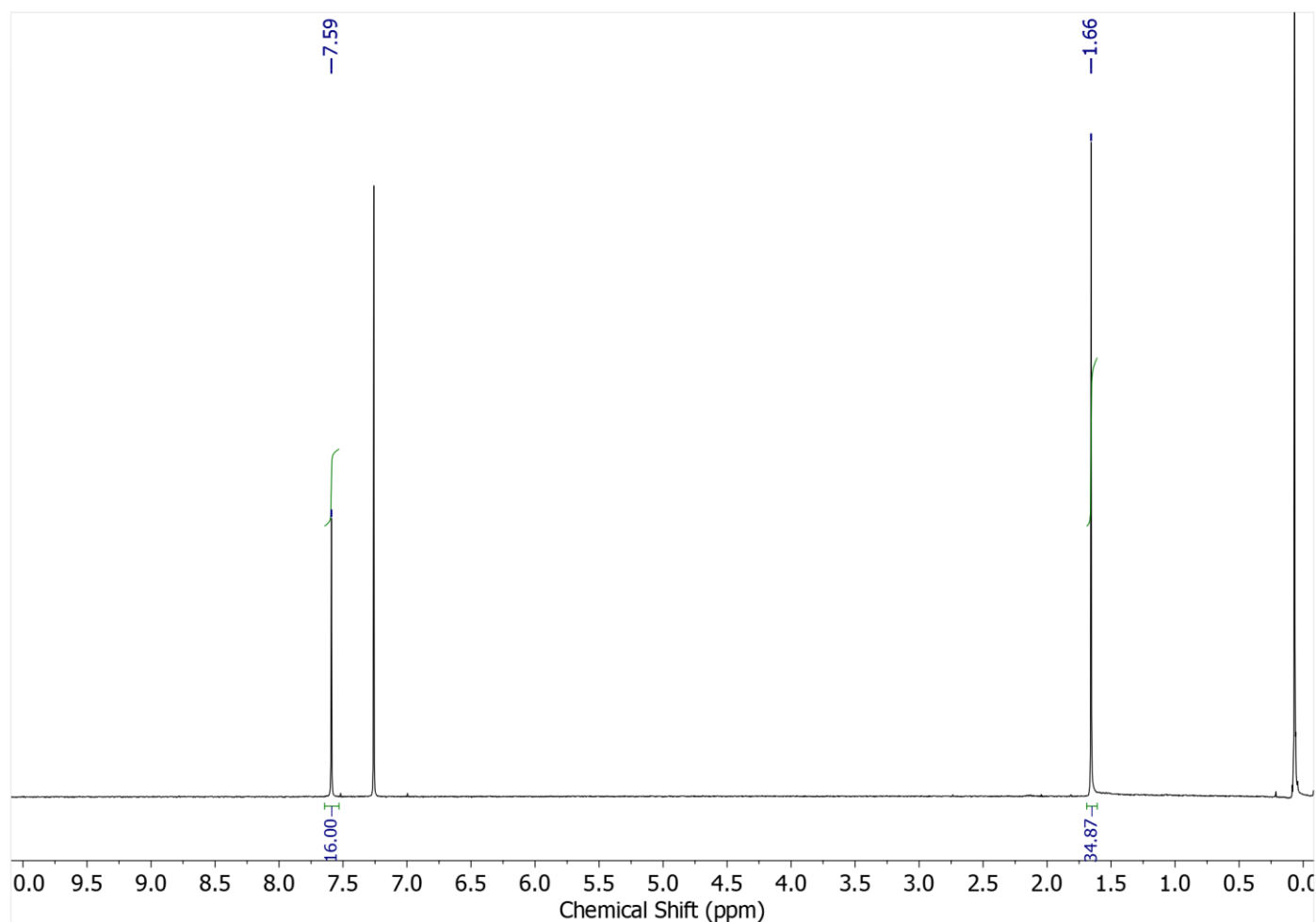


**Figure S5:**  $^1\text{H}$  NMR of SqTI-tBu in  $\text{CDCl}_3$  at 298 K.

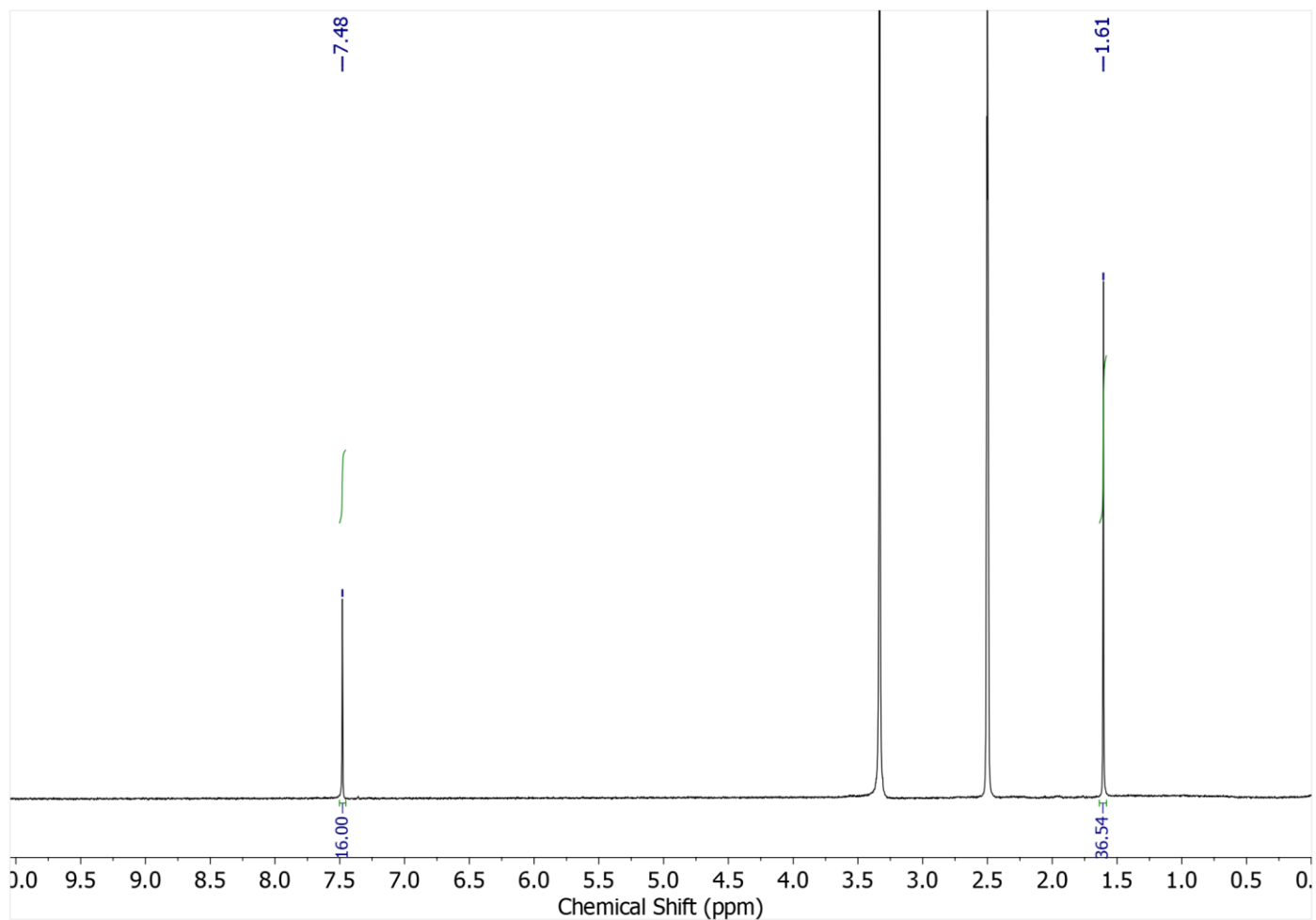


Figure S6:  $^1\text{H}$  NMR of SqTI-tBu in  $\text{DMSO-}d_6$  at 298 K.

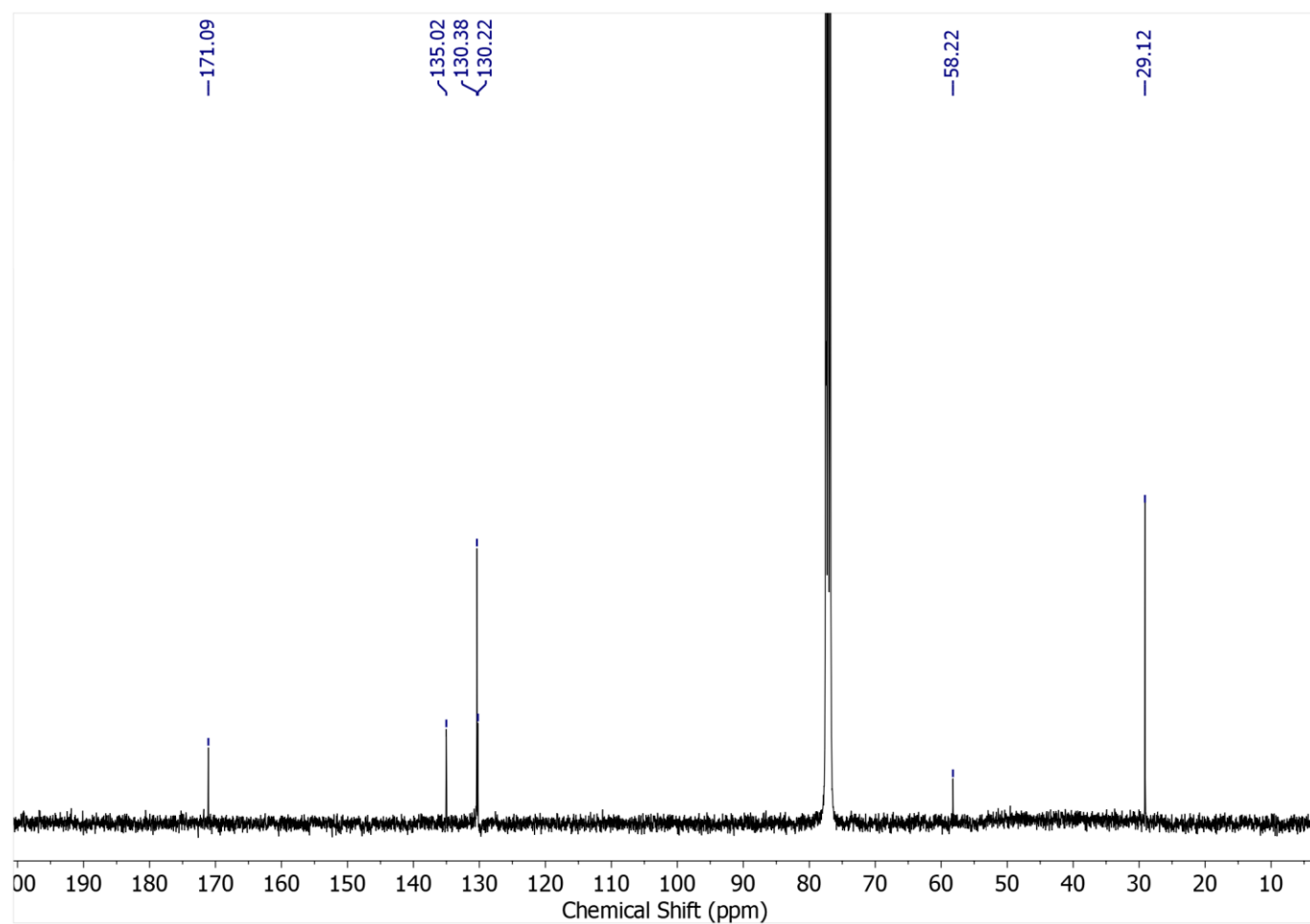
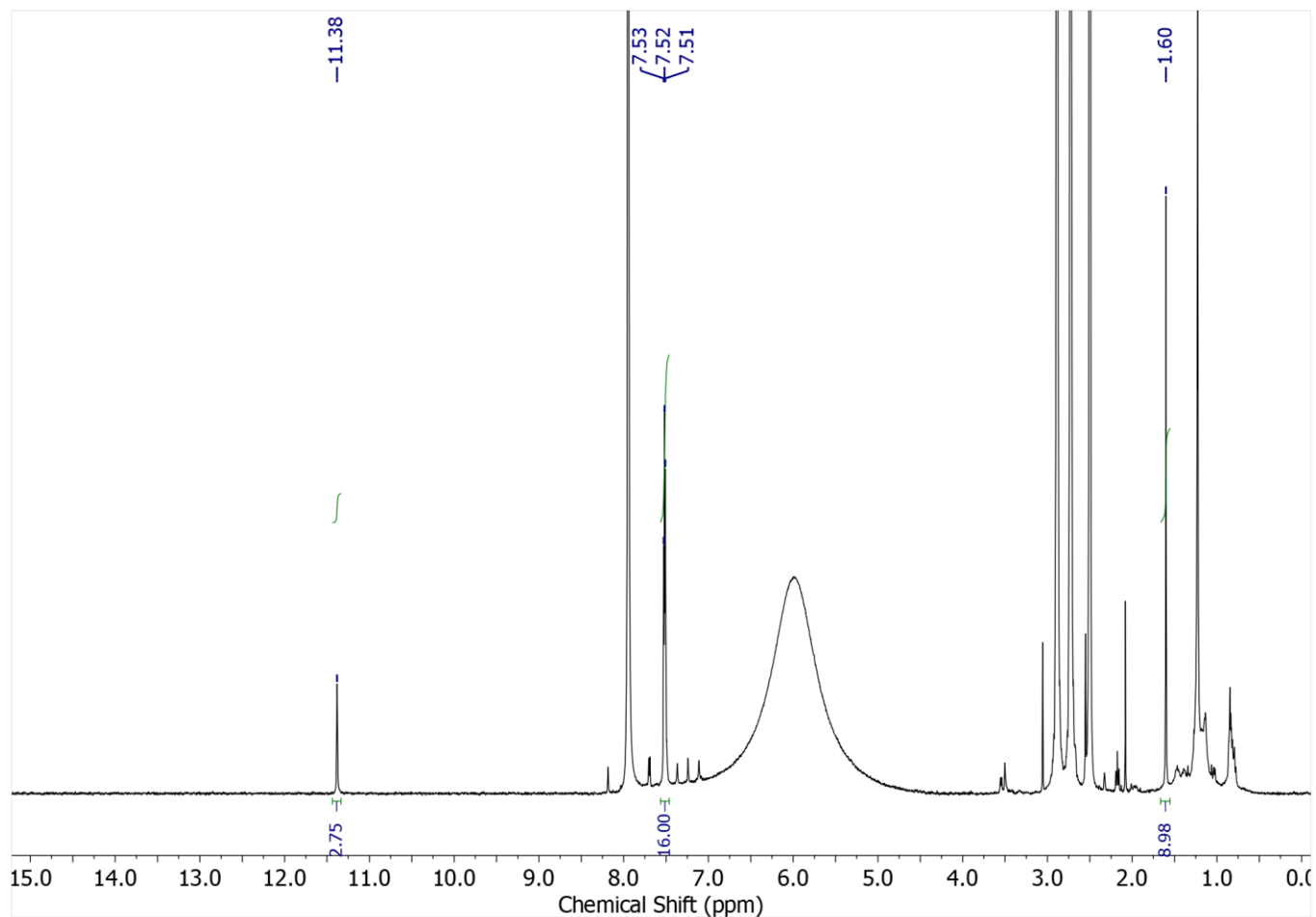
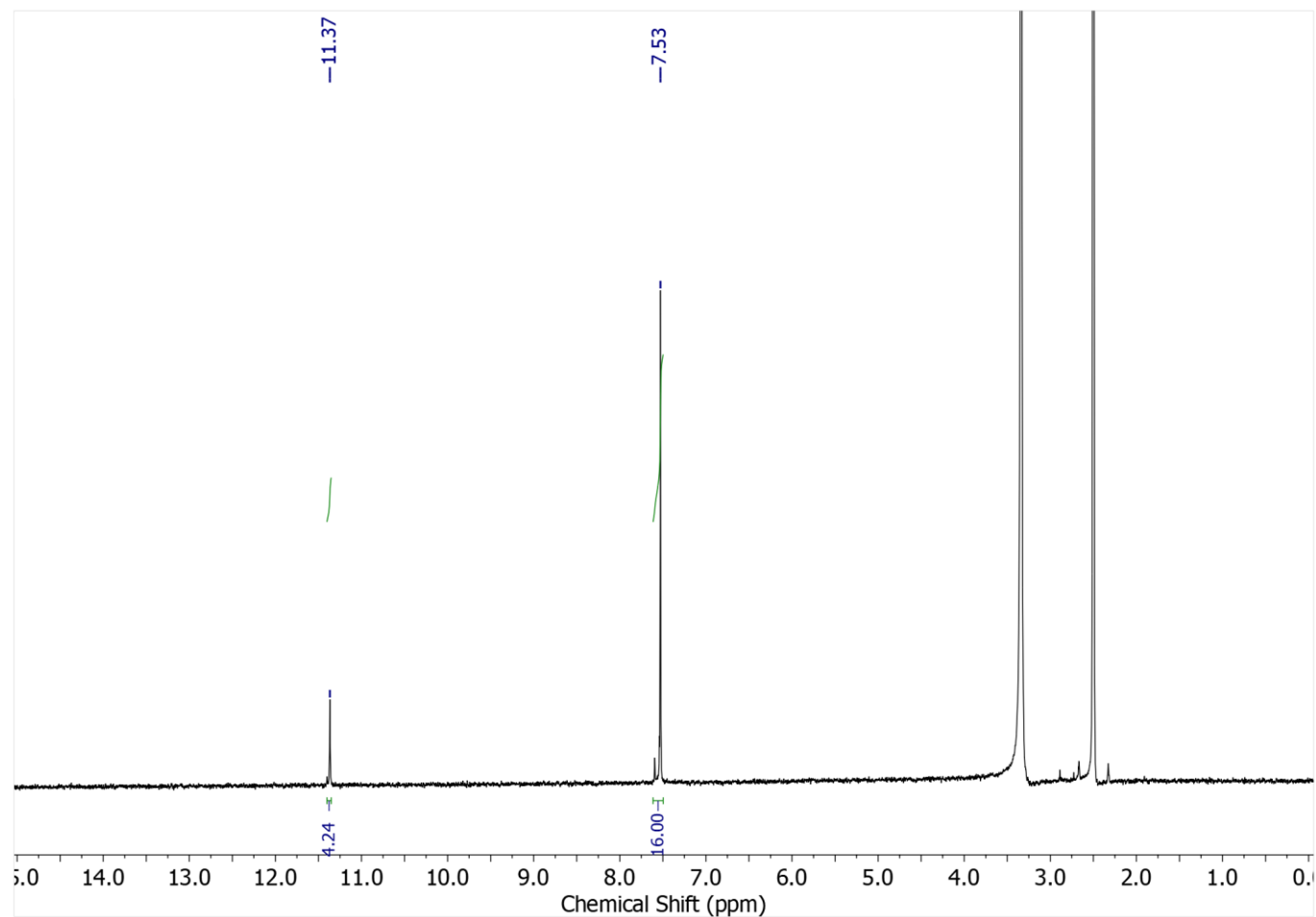


Figure S7:  $^{13}\text{C}\{^1\text{H}\}$  NMR of SqTI-tBu in  $\text{CDCl}_3$  at 298 K.



**Figure S8:**  $^1\text{H}$  NMR of SqTI-tBu after attempted acidic sidechain cleavage by overnight refluxing in trifluoroacetic acid, in  $\text{DMSO-}d_6$  at 298 K.



**Figure S9:**  $^1\text{H}$  NMR of SqTI-H in  $\text{DMSO-}d_6$  at 298 K.

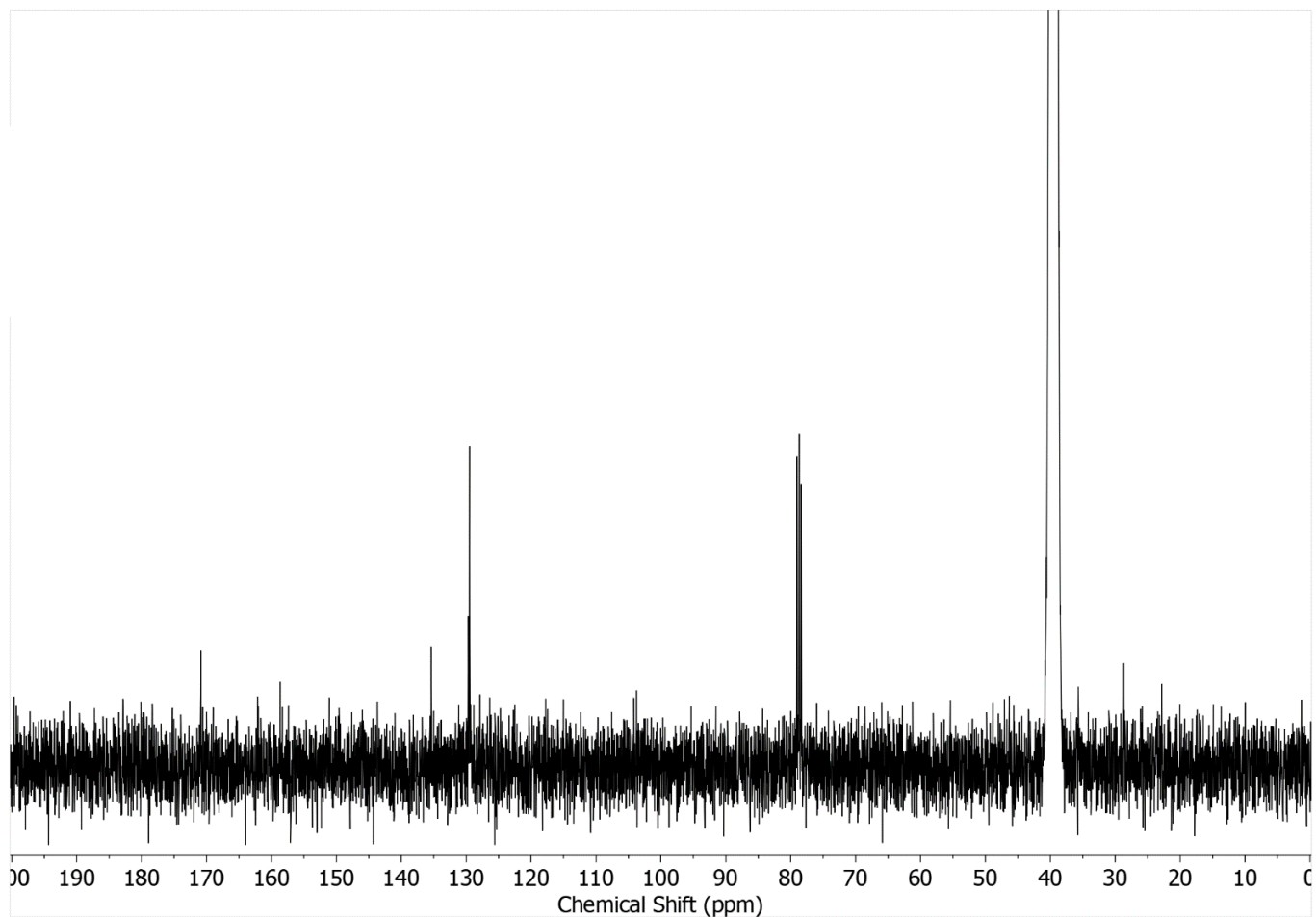


**Figure S10:**  $^{13}\text{C}\{^1\text{H}\}$  NMR SqTI-H in  $\text{DMSO-}d_6$  at 333 K.

### HIGH-RESOLUTION MASS SPECTROMETRY (HRMS)

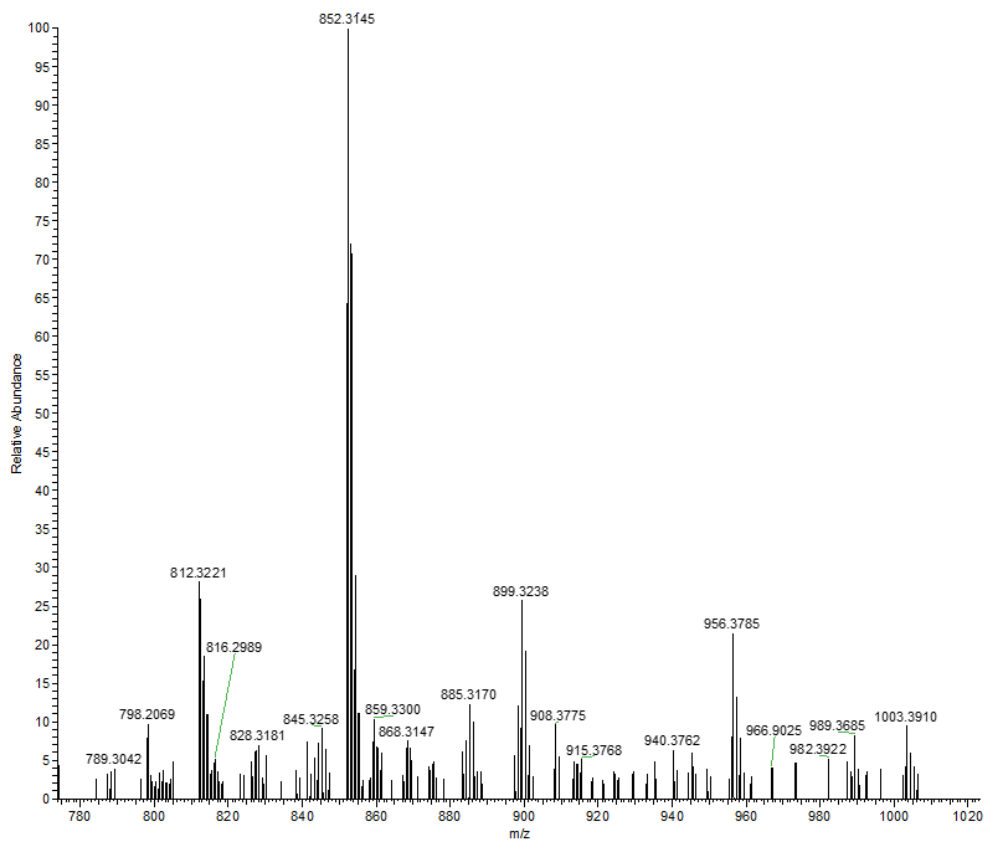


**Figure S11:** HRMS trace of SqTI-iP.

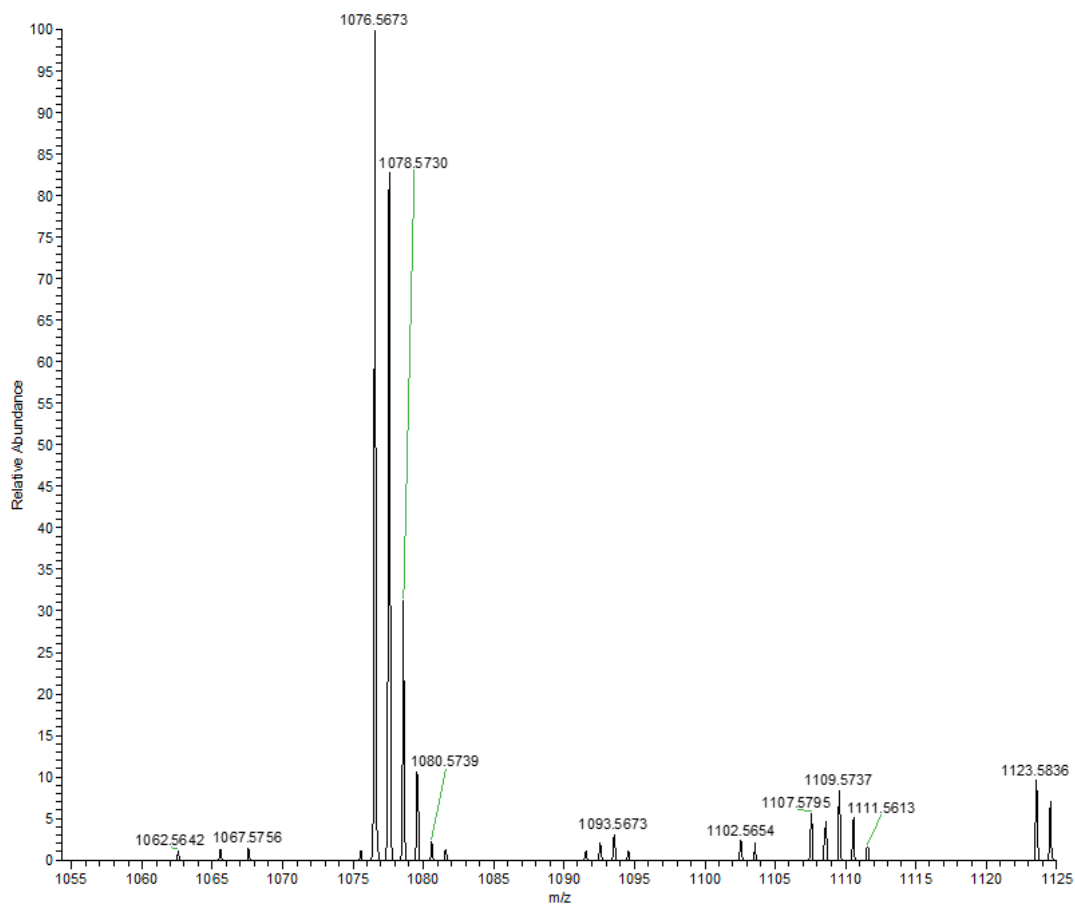


Figure S12: HRMS trace of SqTI-Hp.

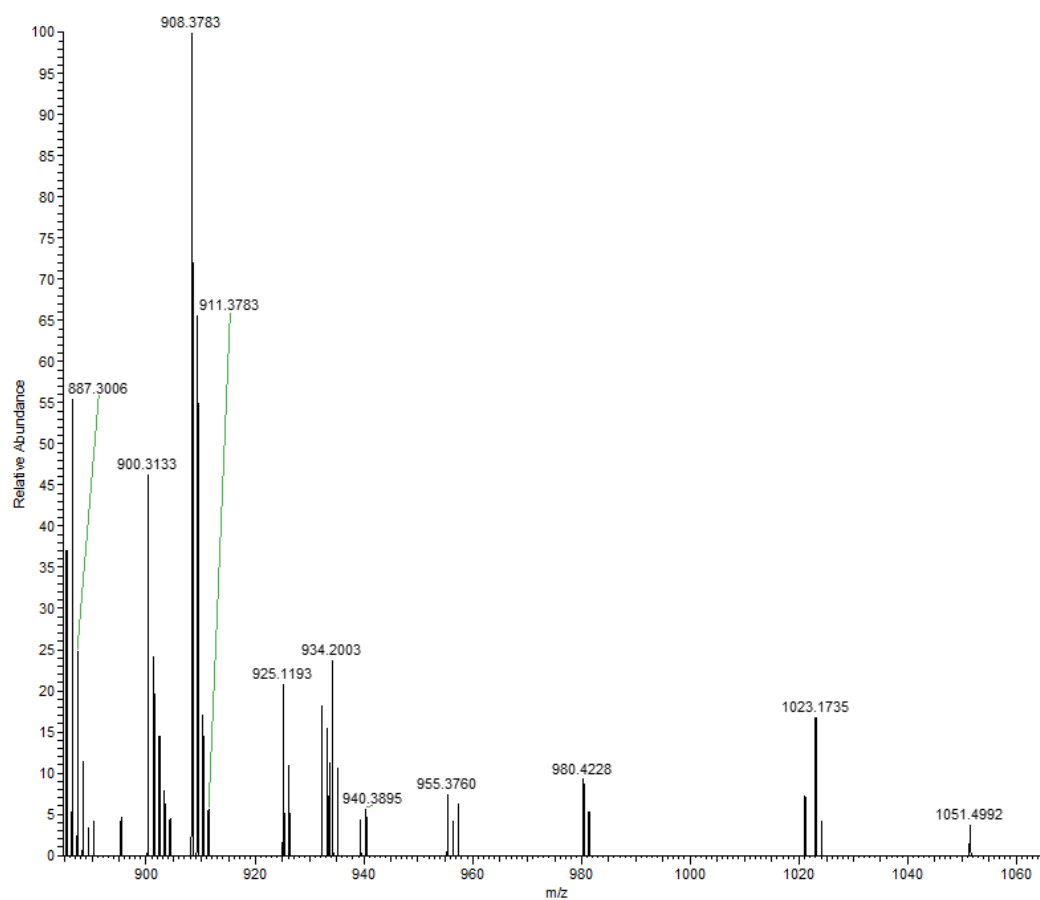
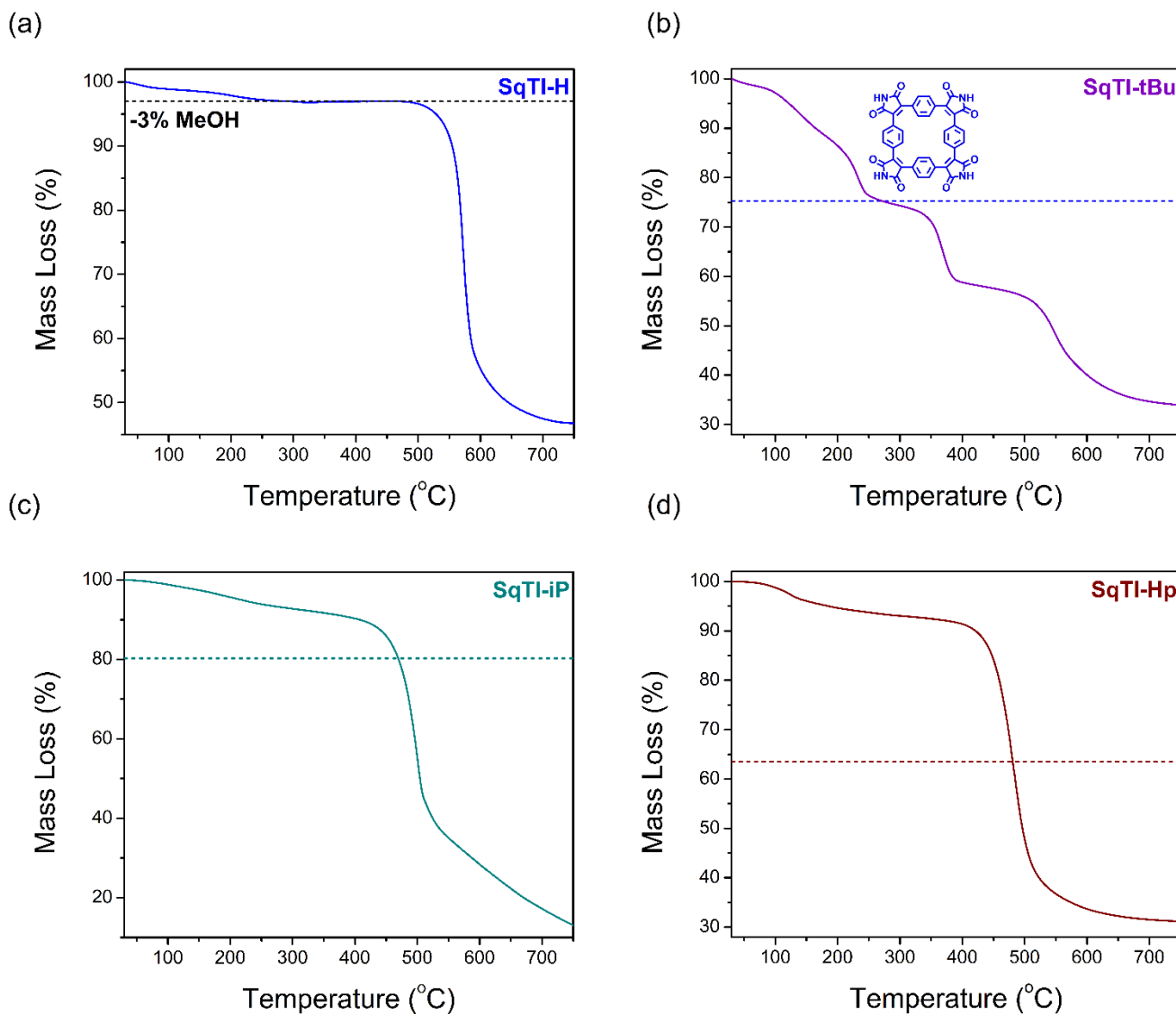


Figure S13: HRMS trace of SqTI-tBu.

## THERMOGRAVIMETRIC ANALYSIS (TGA)

Thermogravimetric analyses (TGA) were performed on a Mettler Toledo TGA at a heating rate of  $10\text{ }^{\circ}\text{C min}^{-1}$ , under a constant stream of  $\text{N}_2$  at a flow rate of *ca.*  $50\text{ mL min}^{-1}$ .



**Figure S14:** TGA traces of (a) SqTI-H (blue) with dashed line showing 3% mass loss attributed to removal of MeOH, (b) SqTI-tBu (violet) with blue dashed line showing ~25% mass loss possibly linked to formation of unsubstituted SqTI, (c) SqTI-iP (dark cyan) with dark cyan dashed line denoting ~20% mass loss predicted to correspond with formation of unsubstituted SqTI (not observed), and (d) SqTI-Hp (burgundy) with burgundy dashed line denoting ~37% mass loss predicted to correspond with formation of unsubstituted SqTI (not observed).

## INFRARED (IR) SPECTROSCOPY

Solid state total reflectance ATR-IR spectra were obtained on an Agilent CARY 630 FTIR spectrometer.

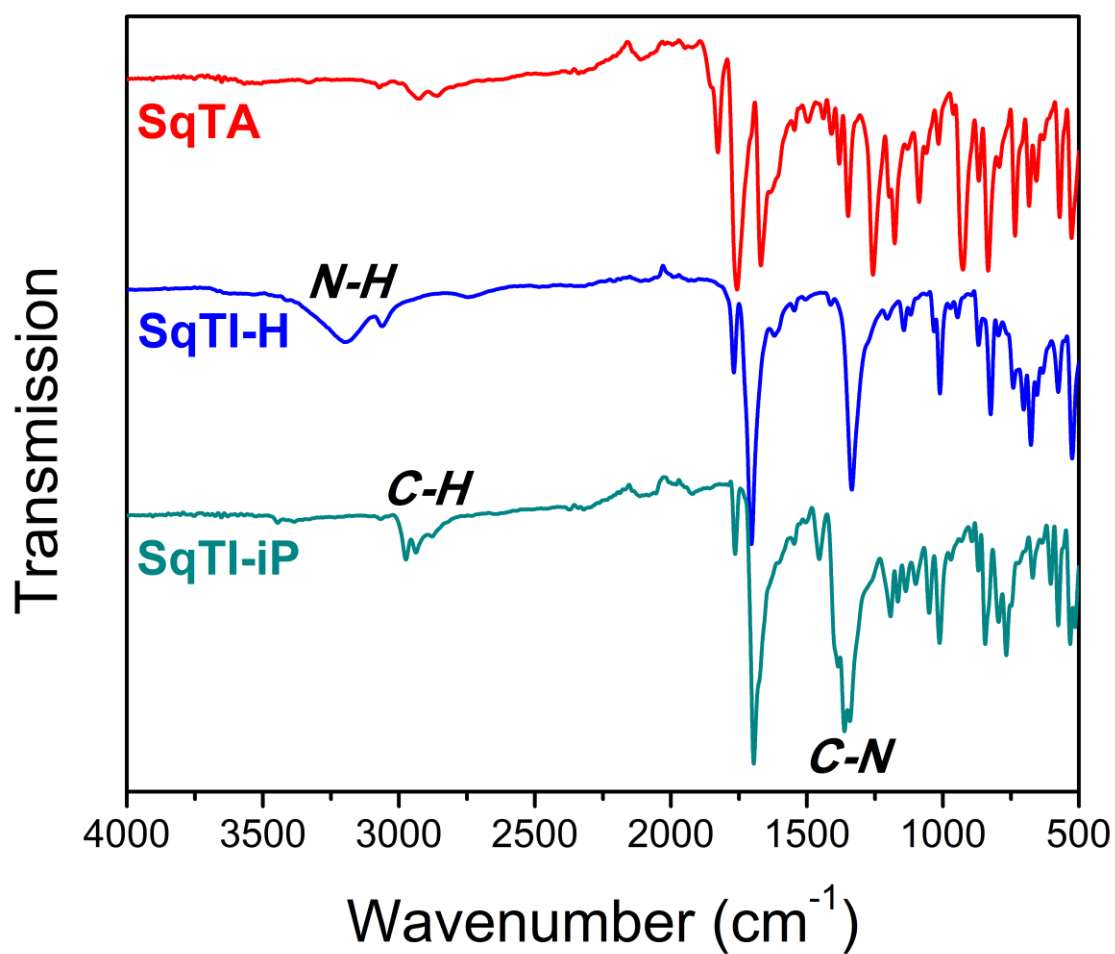


**Figure S15:** ATR-IR of SqTA (red), SqTI-H (blue) and SqTI-iP (dark cyan), with labelling of N-H stretching at 3200  $\text{cm}^{-1}$  for SqTI-H, alkyl C-H stretching between 2800 – 3000  $\text{cm}^{-1}$  for SqTI-iP as well as C-N stretching at 1340  $\text{cm}^{-1}$  for both SqTI-H and SqTI-iP.

## POWDER X-RAY DIFFRACTION (PXRD)

Powder X-ray diffraction (PXRD) data were collected with a Bruker D2 Phaser Diffractometer producing Cu-K $\alpha$  ( $\lambda = 1.5418 \text{ \AA}$ ) radiation, fitted with an SSD 160 detector.

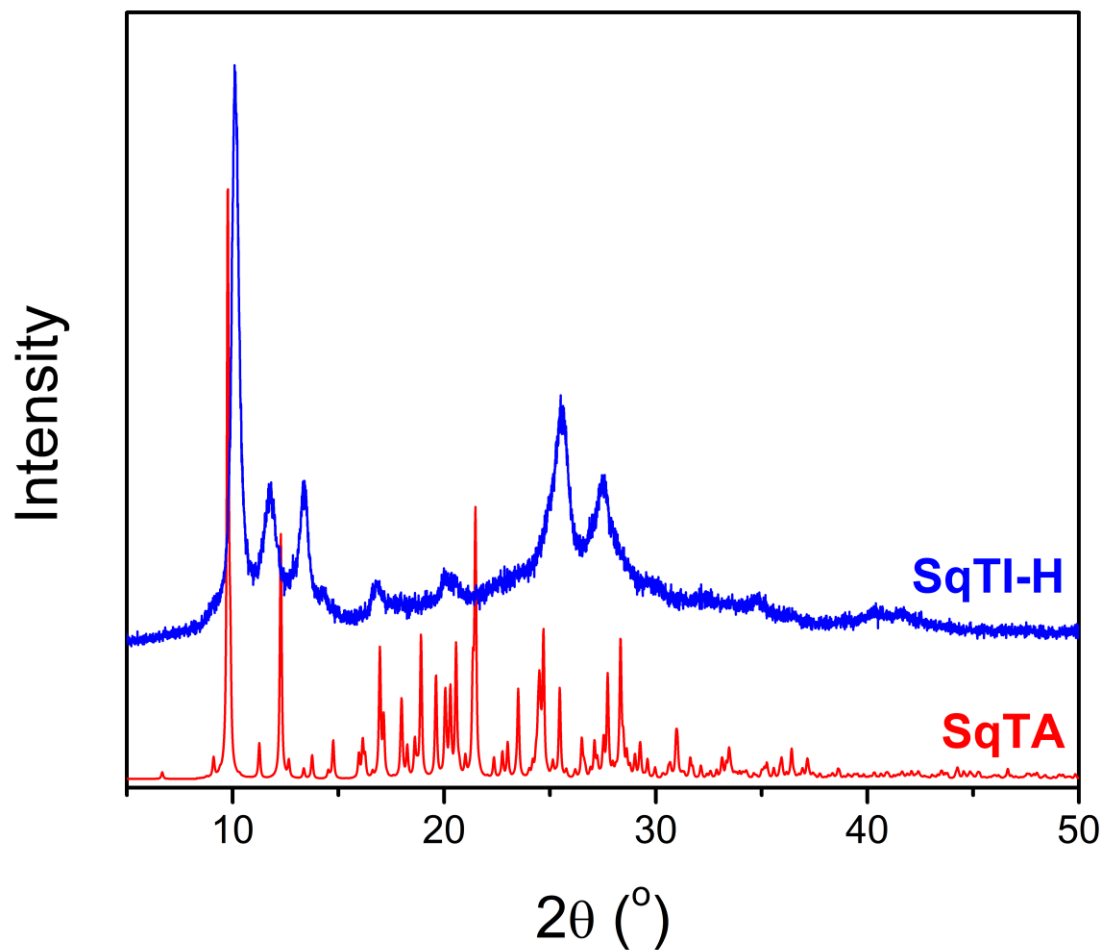


**Figure S16:** PXRD pattern of SqTI-H (blue), as compared to the predicted pattern of SqTA (red) from its single crystal X-ray diffraction structure.<sup>1</sup>

## DIFFERENTIAL SCANNING CALORIMETRY (DSC)

Differential scanning calorimetry (DSC) traces between 40 – 300 °C were collected on a Mettler DSC822e differential scanning calorimeter, at a heating rate of 10 °C/min under a N<sub>2</sub> environment.

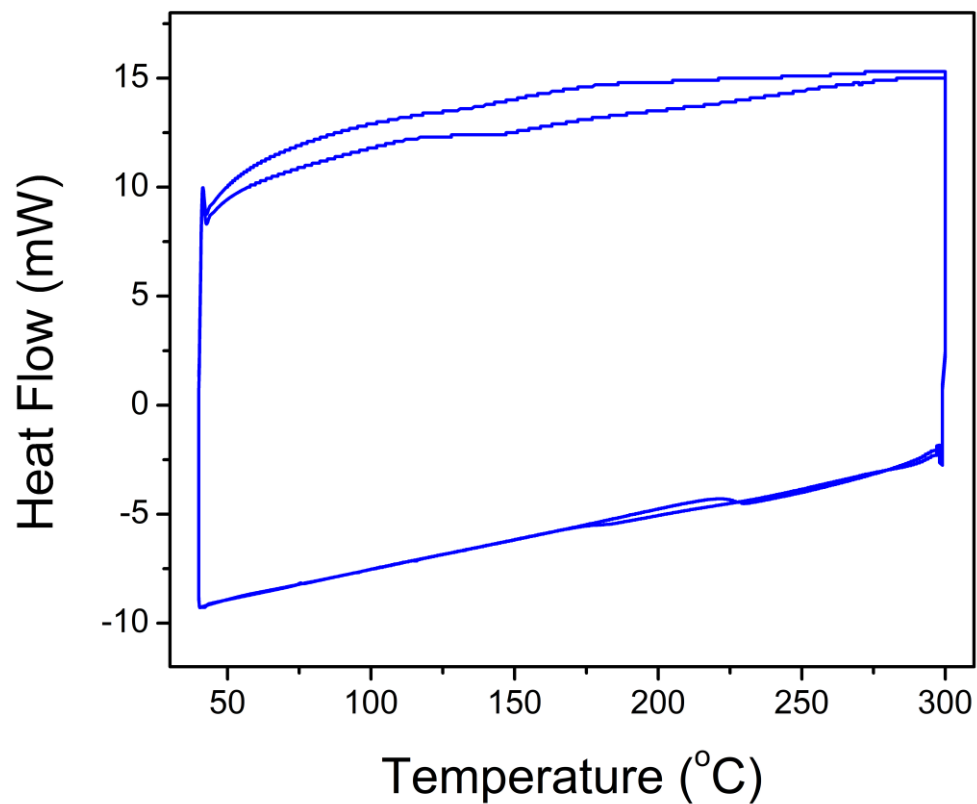


**Figure S17:** DSC trace (2 cycles) of SqTI-H between 40 to 300 °C.

## LITHIUM-ION BATTERY ELECTRODE PERFORMANCE

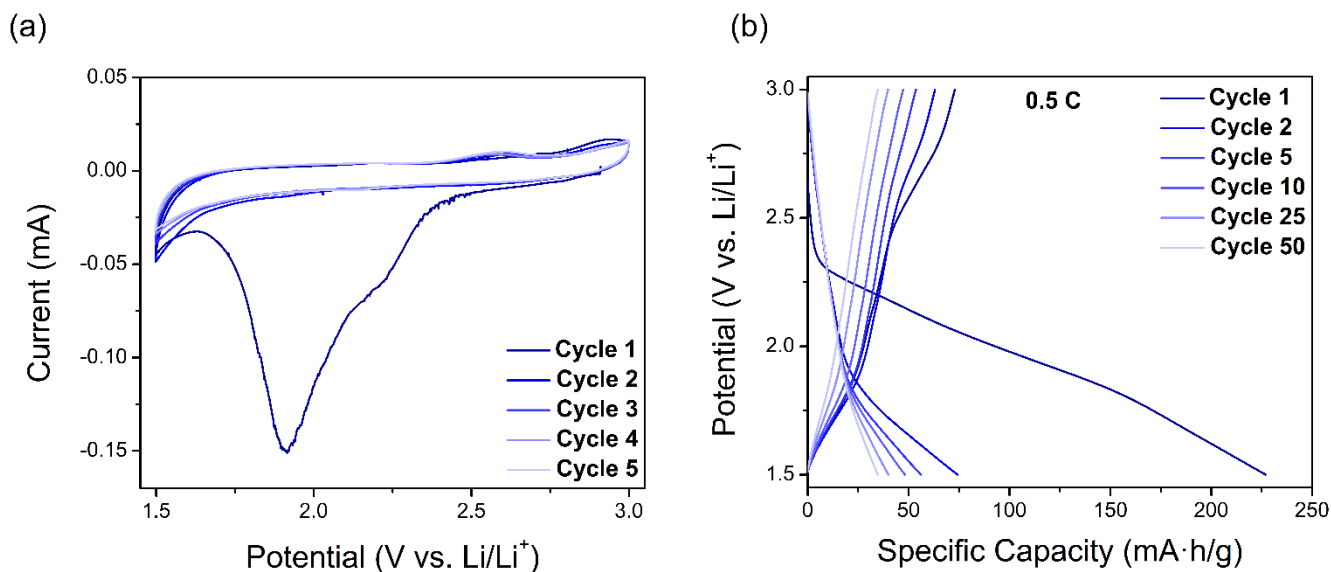


**Figure S18:** SqTI-H composite electrode performance in 1 M LiTFSI/1:1 1,3-dioxolane (DOL) and 1,2-dimethoxyethane (DME) showing (a) cycling voltammograms and (b) charge/discharge profiles at 50 mA/g (0.5 C) constant current cycling.

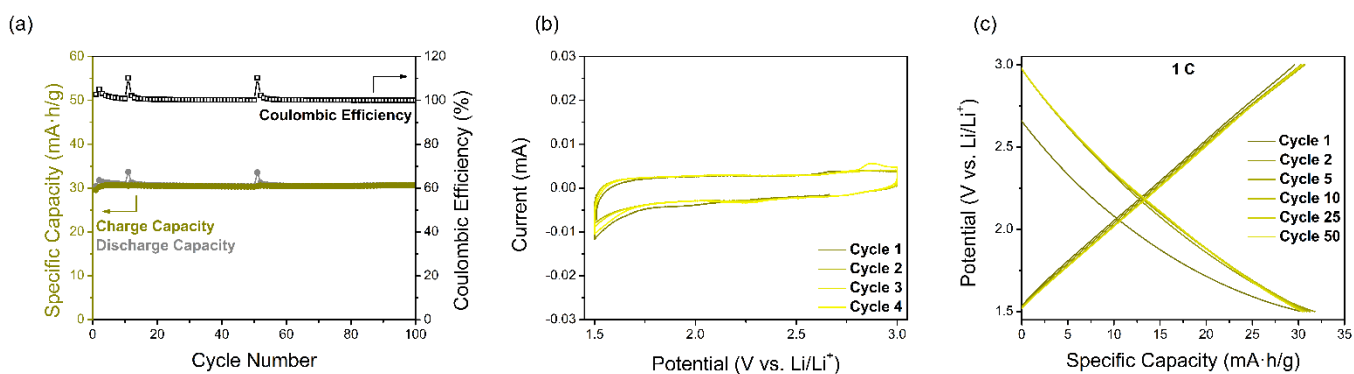


**Figure S19:** Ketjen Black electrode performance in 1 M LiTFSI/1:1 DOL+DME showing (a) cycling performance and coulombic efficiency, (b) cycling voltammograms and (c) charge/discharge profile at 100 mA/g (1C) constant current cycling.

## REFERENCE

1. Eder, S.; Ding, B.; Thornton, D. B.; Sammut, D.; White, A. J. P.; Plasser, F.; Stephens, I. E. L.; Heeney, M.; Mezzavilla, S.; Glöcklhofer, F., *Angew. Chem. Int. Ed.* **2022**, *61*, e202212623.